Supporting Information

Zhang *et al.* 10.1073/pnas.0808573106

SI Methods

Preparation of 70S Ribosomes and RNCs. 70S empty ribosomes were purified from *E. coli* MRE600 following a modified protocol described by Moazed and Noller (1). Cell pellet from a 1-L culture was resuspended in 30 ml buffer A [20 mM Tris·HCl (pH 7.0 at 21 °C), 10.5 mM $MgCl_2$, 100 mM NH_4Cl, 0.5 mM EDTA, 6 mM 2-mercaptoethanol (β-ME)]. The cell resuspension was passed through the French Press twice to lyse the cells. The lysate was clarified by two rounds of centrifugation at 20,000 × *g* for 15 min at 4 °C. The supernatant was layered on a 1.1-M sucrose cushion in buffer B [20 mM Tris·HCl (pH 7.0 at 21 °C), 10.5 mM $MgCl_2$, 500 mM NH_4Cl, 0.5 mM EDTA, 6 mM β-ME, and 1.1 M sucrose] and ultracentrifuged at 100,000 × *g* for 21 h at 4 °C. The ribosome pellet was collected and dissolved in buffer A containing 500 mM NH_4Cl. The dissolved ribosomes were ultracentrifuged at 4 °C for 3 h at 100,000 × *g*. The pellet was dissolved in buffer C [20 mM Tris·HCl (pH 7.0 at 21 °C), 6 mM $MgCl_2$, 100 mM NH_4Cl, and 6 mM β-ME], layered on top of 32 ml sucrose gradients [10–40% (w/v) sucrose in buffer C], and ultracentrifuged at 50,000 × *g* for 14 h at 4 °C. Fractions containing 70S ribosomes were collected and ultracentrifuged at 100,000 × *g* for 17 h at 4 °C. Ribosome pellets were collected and dissolved in storage buffer [20 mM Tris·HCl (pH 7.0 at 21 °C), 10 mM $MgCl_2$, 100 mM NH_4Cl, and 6 mM β-ME]. Ribosomes were stored at −80 °C.

The RNC was generated from *in vitro* translation in a membrane-free cell extract prepared from *E. coli* MRE600 as described (2). I*n vitro* translation was performed at 37 °C for 25 min. The translation mix was layered onto a 40 ml sucrose gradient in buffer S1 [10–50% (w/v) sucrose in 50 mM HEPES-KOH (pH 7.5 at 4 °C), 100 mM $Mg(OAc)_2$, 100 mM NH_4Cl] and ultracentrifuged at 4 °C for 15 h at 23,500 rpm using a SW-32 rotor (Beckman). Fractions containing monoribosome were collected and loaded onto a 1-mL Strep-Tactin Sepharose column (IBA) equilibrated with buffer S1 at 4 °C. Buffer S1 containing 2.5 mM desthiobiotin (Sigma) was used to elute RNCs from affinity column. RNC-containing fractions were centrifuged at 55,000 rpm for 3 h at 4 °C using a TLA-55 rotor (Beckman). Pellets were collected and dissolved in buffer S1 with 25 mM $Mg(OAc)_2$.

1. Moazed D, Noller HF (1989) Interaction of tRNA with 23S rRNA in the ribosomal A, P, and E sites. *Cell* 57:585–597.
2. Schaffitzel C, Ban N (2007) Generation of ribosome nascent chain complexes for structural and functional studies. *J Struct Biol* 158:463–471.
3. Shan SO, Stroud RM, Walter P (2004) Mechanism of association and reciprocal activation of two GTPases. *PLoS Biol* 2:1572–1581.
4. Zhang X, Kung S, Shan SO (2008) Demonstration of a multistep mechanism for assembly of the SRP·SRP receptor complex: Implications for the catalytic role of SRP RNA. *J Mol Biol* 381:581–593.
5. Shan SO, Chandrasekar S, Walter P (2007) Conformational changes in the GTPase modules of the signal reception particle and its initiation of protein translocation. *J Cell Biol* 178:611–620.

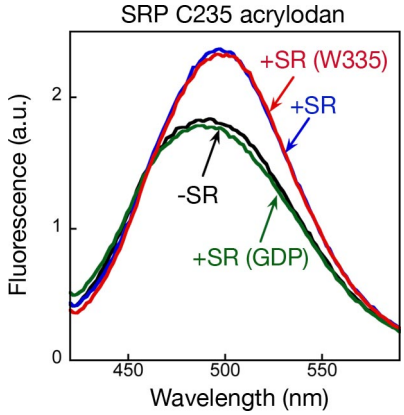

Fig. S1. Acrylodan labeled SRP C235 monitors formation of the *closed/activated* conformation. Fluorescence emission spectra are acquired in the presence of GppNHp for acrylodan-labeled SRP C235 alone (0.1 μM; black), labeled SRP C235 incubated with 1 μM wild-type SR (blue), or labeled SRP C235 incubated with 1 μM SR A335W (red), which is blocked in the *closed→activated* rearrangement and thus isolates the *closed* complex (3), or in the presence of GDP with 10 μM SR (green), which isolates the *early* complex (4).

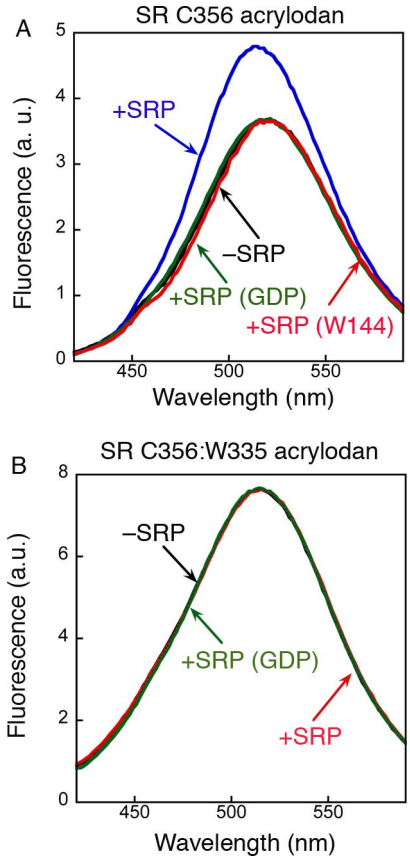

Fig. S2. Acrylodan labeled SR C356 specifically monitors formation of the *activated* SRP·SR complex. (*A*) Fluorescence emission spectra was obtained for acrylodan labeled SR C356 alone (0.1 μM; black), acrylodan-labeled SR C356 incubated with wild-type SRP (blue) or SRP A144W (red) in the presence of GppNHp, or with 10 μM SRP in the presence of GDP (green). SRP A144W allows a stable *closed* complex to form but specifically blocks formation of the *activated* complex (5). The absence of fluorescence change with SRP A144W shows that acrylodan-labeled SR C356 specifically monitors formation of the *activated* complex. (*B*) Acrylodan-labeled C356 does not change fluorescence if mutant SR A355W (3) was used to block the formation of the *activated* complex. Spectra was obtained for 0.1 μM acrylodan-labeled SR A335W:C356 alone (black) and when this labeled SR mutant was incubated with 1 μM SRP in the presence of GppNHp (red) or with 5 μM SRP in the presence of GDP (green). The absence of a fluorescence change shows that the probe on SR T356 does not detect the *early* or the *closed* complex.

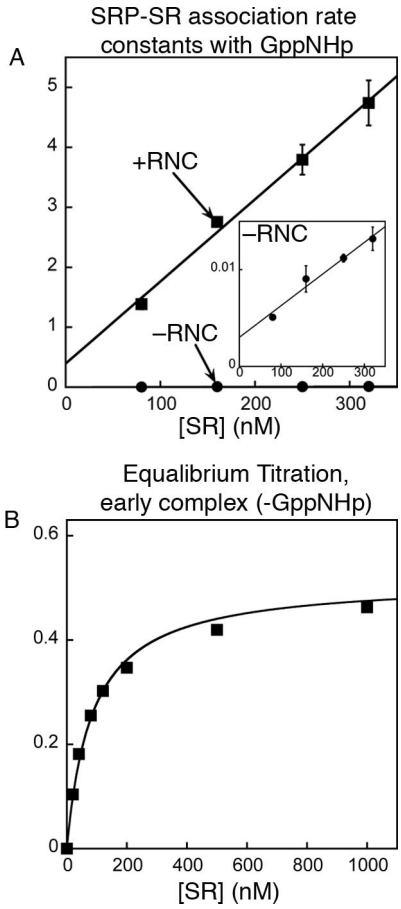

Fig. S3. Full-length FtsY behaves similarly to FtsY (47–497) in its ability to respond to the cargo. (*A*) Cargo accelerates SRP-SR complex assembly with GppNHp by 400-fold when full-length FtsY is used. The data were obtained with 20 nM SRP, 100 μM GppNHp, and varying concentrations of full-length FtsY in the presence and absence of 60 nM RNC. The data were analyzed as in Fig. 2*B* and give association rate constants (k_{on}) of $1.3 \pm 0.1 \times 10^7$ $M^{-1}{\cdot}s^{-1}$ and $3.3 \pm 0.5 \times 10^4$ $M^{-1}{\cdot}s^{-1}$ with (■) and without (●) 60 nM RNC, respectively. (*B*) The *early* complex formed with full-length FtsY is stabilized significantly by the cargo, as was observed with FtsY (47–497). Equilibrium titration of the *early* complex was carried out in the absence of GppNHp with 50 nM RNC. Nonlinear fits of data gave K_d values of 85 ± 5 nM, which is comparable to the value of 80 ± 4 nM obtained with FtsY (47–497) (Fig. 3*B*, squares).

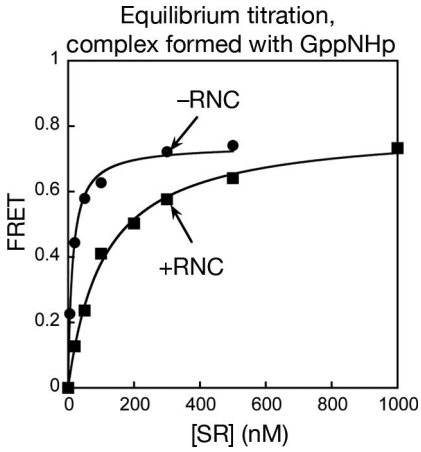

Fig. S4. Equilibrium titration of the SRP-SR complex assembled in GppNHp with (■) and without (●) RNC using the FRET assay. Nonlinear least squares fits of data gave K_d values of 14 ± 3 nM (without RNC) and 60 ± 7 nM (with RNC). For the cargo-loaded SRP, an accurate determination of the stability of the *closed/activated* states by FRET is complicated by the fact that the stabilities of the SRP-SR complexes assembled with and without GppNHp are very similar (60 vs. 80 nM, respectively); thus, a significant fraction of the SRP•SR complex is in the *early* conformation even in the presence of GppNHp. The observed affinity of the cargo·SRP·SR complex of 60 nM is consistent with the weighted average of the stabilities of the *early* intermediate (80 nM, Fig. 4*C*) and the *closed* complex (40 nM, Fig. 4*C*) that are equally populated in the presence of GppNHp and cargo.

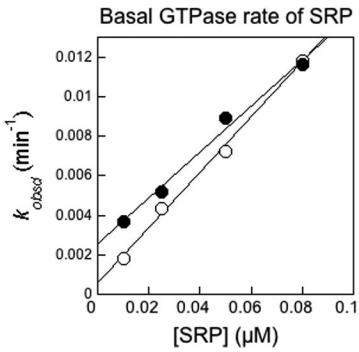

Fig. S5. The RNC does not significantly affect the basal GTPase reaction of the free SRP. The basal GTPase reactions were carried out under single turnover conditions with trace γ-^{32}P-GTP ($<$ 0.1 nM) and varying concentrations of SRP. Linear fits of the data give k_{cat}/K_m values of 1.4×10^5 M^{-1}·min^{-1} and 1.2×10^5 M^{-1}·min^{-1} in the absence (●) and presence of RNC (○), respectively.

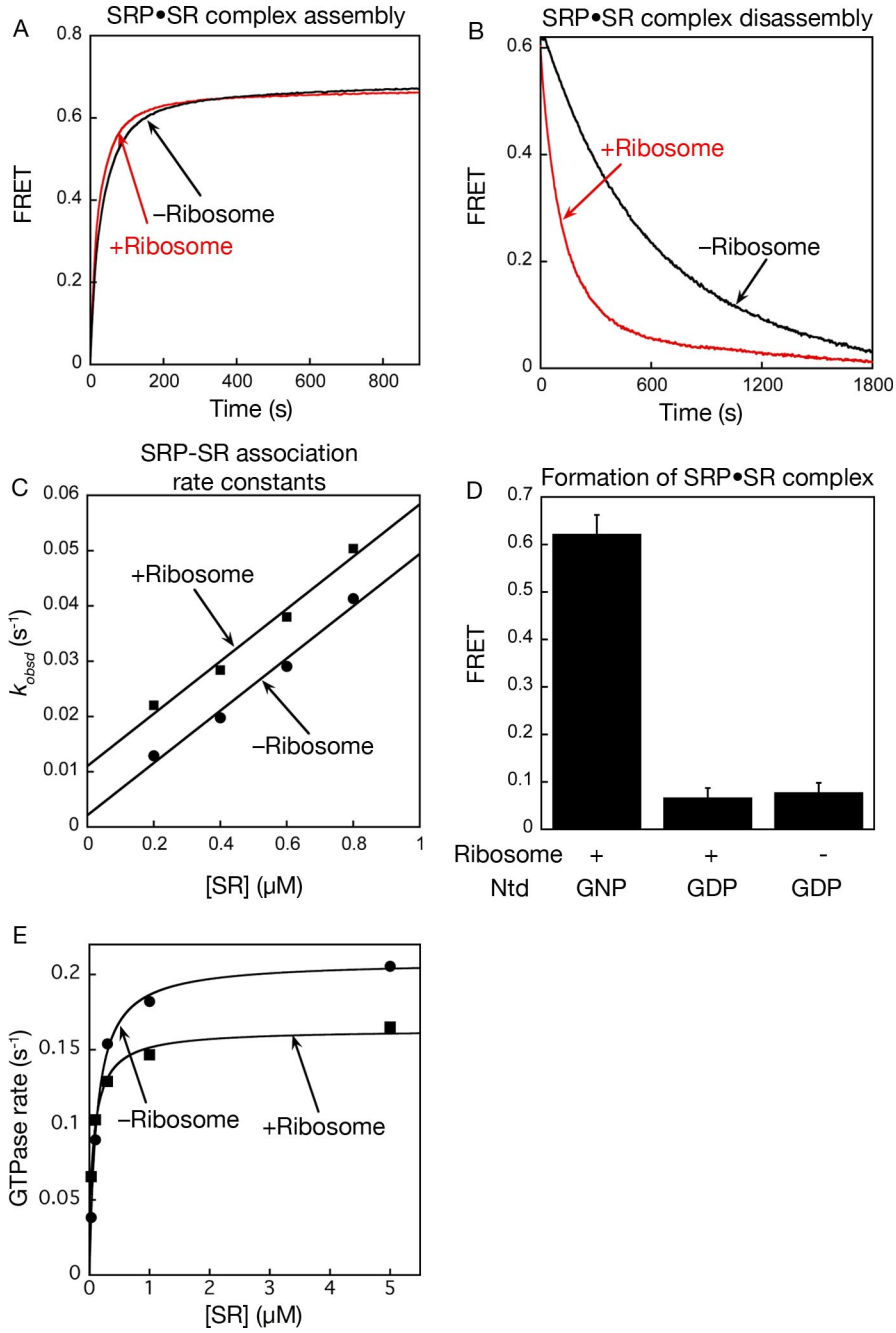

Fig. S6. Empty ribosomes do not substantially alter the interaction between the SRP and SR. (*A*) The time course for SRP-SR complex formation, monitored by FRET, in the absence (black) and presence (red) of 0.8 μM ribosomes. Data were obtained with 0.1 μM SRP, 1.0 μM SR, and 100 μM GppNHp. (*B*) The ribosome accelerates disassembly of the SRP-SR complex approximately 4-fold. The rate constants for complex disassembly were determined in the absence (black) and presence (red) of 1.0 μM ribosomes. Fits of the data to single exponential decay give dissociation rate constants of 0.010 $\pm$ 0.003 s^{-1} and 0.0027 $\pm$ 0.004 s^{-1} in the presence and absence of ribosome, respectively. (*C*) The ribosome does not affect the rate of SRP-SR complex assembly. Association kinetics of the SRP·SR complex was measured as in Fig. 2 with (■) or without (●) 1.0 μM ribosome. Linear fits of the data gave k_{on} values of (4.7 $\pm$ 0.7) $\times$ 10^4 $M^{-1}\cdot s^{-1}$ with ribosome and (4.7 $\pm$ 0.4) $\times$ 10^4 $M^{-1}\cdot s^{-1}$ without ribosome, and k_{off} values of 0.011 $\pm$ 0.004 s^{-1} with ribosome and 0.0022 $\pm$ 0.003 s^{-1} without ribosome. (*D*) Ribosome does not stabilize the *early* intermediate. FRET values are compared for SRP-SR *early* complex assembled with GDP in the presence and absence of ribosome. Data were obtained with 0.1 μM SRP, ribosome, and 1.0 μM SR. GNP denotes GMPPNP. (*E*) Ribosome does not substantially affect the stimulated GTP hydrolysis in the SRP•SR complex. GTPase rate constants were measured and analyzed as described in *SI Methods* using 15 nM SRP and 50 μM GTP in the absence (●) and presence (■) of 1.0 μM ribosome.